International Journal of Nanoelectronics and Materials
IJNeaM
ISSN 1985-5761 | E-ISSN 2232-1535

# A study on physical properties of Coronene oxide as a function of number of oxygen atoms and temperature by density functional theory

Taif Talib Khalaf [a] *, and Mohammed T. Hussein [b]

[a]*Department of Physics, College of Science, University of Baghdad, Baghdad, Iraq*
[b]*Alnukhba University College, Baghdad, Iraq*
*∗Corresponding author. E-mail: taif.taleb1604a@sc.uobaghdad.edu.iq*

Received 25 December 2023, Revised 15 July 2024, Accepted 19 August 2024

**ABSTRACT**

The electronic properties like (HOMO, LUMO levels and Energy gap), and spectroscopic properties (IR spectra) in addition to thermodynamics characteristics like (Gibbs free Energy, Enthalpy, Entropy, and Heat capacity) of Coronene $C_{24}$ and reduced Coronene oxide $C_{24}O_x$ where x=1-5 is a number of oxygen atoms and different temperature from (298 – 398) K were studied. The methodology utilized in this study involved the application of Density Functional Theory (DFT) using the Hybrid functional B3LYP (Becke, 3-parameters, Lee –Yang-Parr) with 6-311G** basis sets. The band gap of Coronene ($C_{24}$) 3.5 eV was calculated, while for reduced coronene oxide $C_{24}O$ - $C_{24}O_5$ has been varied from (1.68 to 0.89) eV due to broken symmetry and adding levels inside the energy gap. The IR intensity of $C_{24}O_5$ increases with increasing temperature between (298 and 398) K because of the number of excited atoms, the spectroscopic properties were compared with experimental results, in particular the Longitudinal Optical (LO) mode of vibration for graphene oxide 1582 $cm^{-1}$ which agreed well. The Gibbs free energy and enthalpy decreased (in the negative sign) with an increased number of oxygen atoms and temperatures which means an exergonic reaction.

**Keywords:** *Coronene oxide, Electronic, Spectroscopic, Thermodynamics properties, DFT*

## 1. INTRODUCTION

Coronene, a polyaromatic hydrocarbon (PAH) molecule characterized by a core ring shared with six surrounding rings, is recognized as a distinctive super benzene molecule. It is naturally present in sedimentary rock and can also be detected during the hydrocracking process in petroleum refining [1-5]. The $sp^2$ carbon structure has garnered significant attention in the synthesis of several π-conjugated organic compounds [6-10]. And further electronic [11]. Coronene is classified as a polycyclic aromatic hydrocarbon (PAH) because of its molecular structure, which consists of six benzene rings that are fused together in a peri arrangement. This unique arrangement allows for the electrons within Coronene to be completely delocalized among the benzene rings. Their unique planar electrical structure allows Coronene molecules to tightly stack, which promotes efficient self-assembly and increased electron mobility [12-17]. Carbon nanotubes and graphene, two materials with remarkable electron conductivity, are thought to represent extensions of the Coronene structure. Several attempts have been made to create Coronene derivatives with a variety of electrical and electronic characteristics [18-24]. The first use of graphene was in the field of electronic devices, focusing on its electronic properties [25-27]. Graphene has been applied in numerous fields, such as energy storage devices like lithium-ion batteries, supercapacitors, gas detection and conducting electrodes [28-30]. Previous studies used Coronene ($C_{24}H_{12}$) as a model to analyze spectroscopic and structural changes in graphene oxide (GO) due to oxygenated groups. Geometry optimization, vibrational IR, and Raman spectra of functionalized Coronene molecules are performed. The results provide valuable data for GO IR and Raman spectra analysis, revealing more detailed structural effects [31]. Studied analysed the molecular structure of Coronene and Coronene-Y molecules using geometrical optimization. It was found that Y atoms interacting with Coronene resulted in new bonds and reduced ionization potential but increased electron affinity. Coronene acted as a donor in Coronene-Y, while Coronene-B and C had an energy gap similar to semiconductors. Coronene-In was the most polarizable molecule, while Coronene-C and Coronene-O were anti-ferromagnetic [32]. Benzene, Coronene, and Circumcoronene of graphene quantum dots (GQDs) with zigzag edges were studied, utilizing the DFT theory and PBE functional, this study examines the alteration of individual properties about the quantity of atoms present in the graphene quantum dots (GQDs), while also noticing both linear and nonlinear fluctuations. This work additionally examines the utilization of Raman spectroscopy in the context of comparing the PBE and B3LYP functional for various sizes of graphene quantum dots (GQDs). Furthermore, the investigation explores the changes observed in the G peak for each function. The calculations were conducted using the Gaussian 09W software tool, employing 3-21G Gaussian basis sets. The results of this study have substantial implications in several disciplines,

such as materials science and the field of energy storage [33]. In our previous study the electronic properties of Coronene ($C_{24}$), reduced Coronene oxide ($C_{24}O_5$) and the interaction between $C_{24}O_5$ and nitrogen dioxide using DFT, and Gaussian view 05 software [34]. Also the electronic characteristics such as band gap HOMO and LUMO level, as well as the spectroscopic properties like IR and Raman spectra of Coronene $C_{24}H_{12}$ after removing hydrogen atoms and substituting with oxygen to get reduced Coronene oxide ($C_{24}O$- $C_{24}O_5$), were studied [35]. In the present work adds the variation of temperature as well as the number of oxygen atoms to give a complete aspect of the electronic, spectroscopic and thermodynamic properties of Coronene $C_{24}$ and Reduced Coronene Oxide $C_{24}O_X$ where x=1-5 which is a very important Nanostructure in optoelectronics devices.

## 2. METHODOLOGY

The DFT is the most dependable technique for comprehending the characteristics and structure of molecules and nanostructures. DFT has gained a reputation because of its strong match to experimental data. Among the most often used DFT methods is B3LYP [36-41]. It was discovered that the B3LYP was better than other functional that encouraged its utilization. Energy from exchange-correlation sources is combined with HF exchange in the hybrid functional B3LYP [42]. For light atoms such as C and O, we will adopt 6-311G** basic states in this investigation [43, 44]. In order to account for the frequency of vibration, scaling factors with a value of 0.967 were employed [45]. The geometric analysis was carried out using Gaussian view 05, while the computations were carried out using Gaussian 09W software [46] as shown in Figure 1.

## 3. RESULTS AND DISCUSSION

### 3.1. Electronic Properties

The energy gap, also known as the band gap, refers to the change in energy levels between the highest occupied molecular orbital (HOMO) and the lowest unoccupied molecular orbital (LUMO) [47].

$$Eg = |LUMO - HOMO| \quad (1)$$

The energy gap (Eg) can be found from differences between the first low unoccupied molecular orbital (LUMO) which is similar to the conduction band (C.B) and the last high occupied molecular orbital (HOMO) which is equal to the valance band (V.B) of Coronene ($C_{24}$) and reduced coronene oxide ($C_{24}O_X$) where (X=1-5) as a function of a number of oxygen atoms as shown in Figure 2 which shows the energy levels (HOMO and LUMO). Figure 3 The energy gap of Coronene $C_{24}$ and reduced coronene oxide $C_{24}O$-$C_{24}O_5$ with fluctuations because of the small number of atoms which are within the computer capabilities compared with the experimental value (1.4) eV for Graphene [48] and a range of (1-2.2) eV for graphene oxide (GO) [49, 50].

The energy band gap of Coronene ($C_{24}$) is determined to be 3.5 eV, primarily attributed to the strong symmetry of the Coronene nanostructure. The band gap of quasiparticles is significantly influenced by both the Coulomb interaction and the quantum confinement geometry [51]. There was a decrease in the energy gap with an increase in the number of oxygen atoms adding to a Coronene ($C_{24}$) because of the symmetry broken and adding level inside of the energy gap.

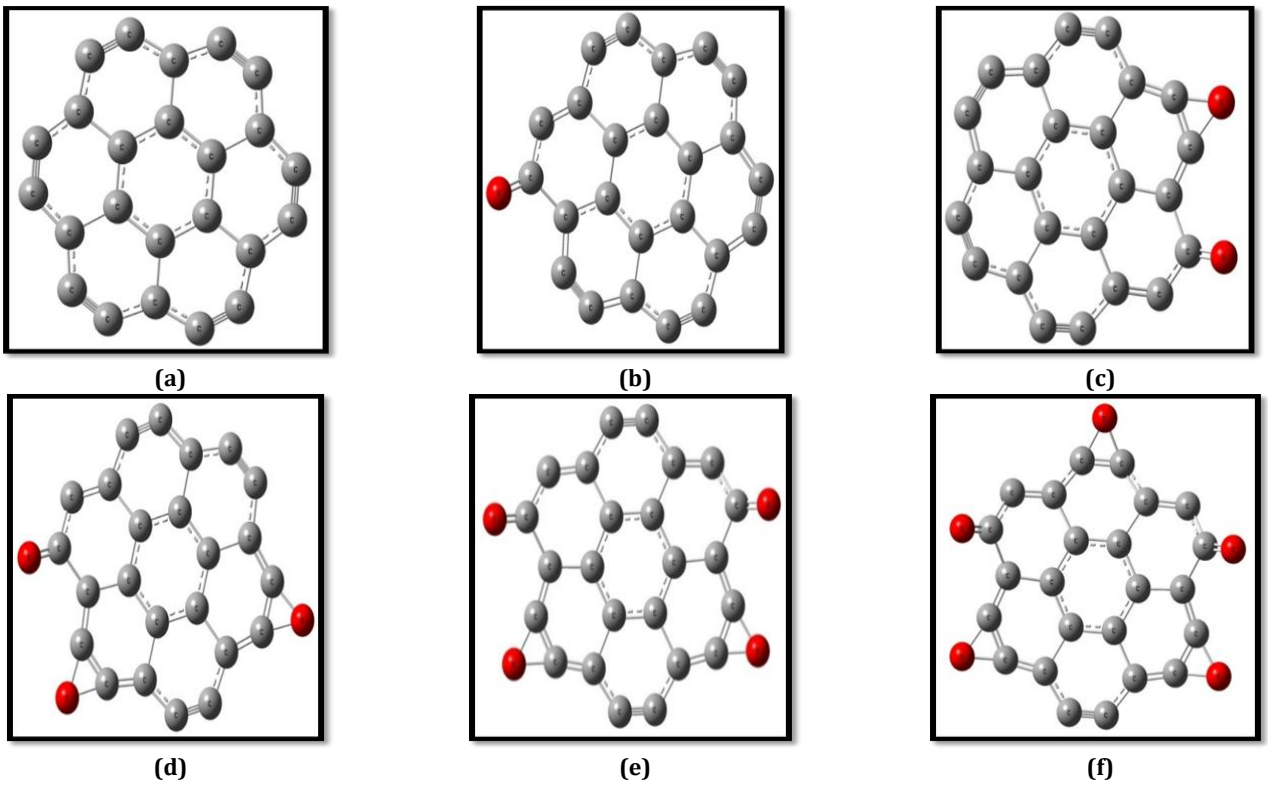


**Figure 1**. Geometrical optimization of (a) Coronene $C_{24}$ and (b, c, d, e, f) reduced Coronene oxide ($C_{24}O$ - $C_{24}O_5$)

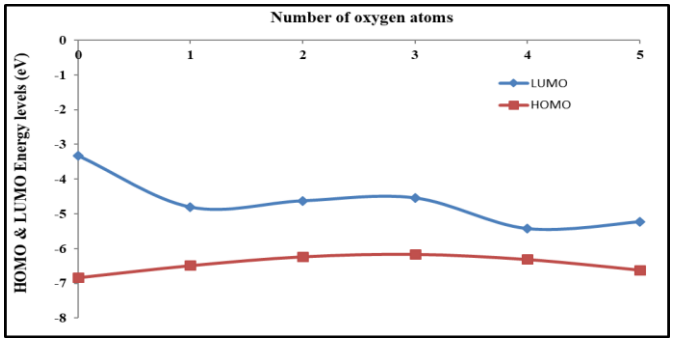


**Figure 2**. Energy levels (HOMO and LUMO) of Coronene $C_{24}$ and reduced Coronene oxide ($C_{24}O$ - $C_{24}O_5$) as a function of a number of oxygen atoms

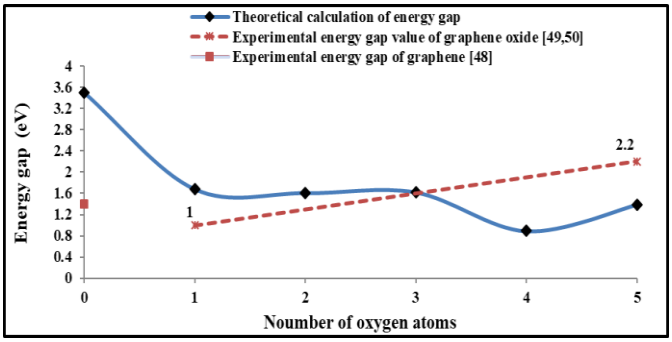


**Figure 3**. The energy gap of Coronene $C_{24}$ and reduced Coronene oxide ($C_{24}O$ - $C_{24}O_5$) according to the oxygen atoms

### 3.2. Thermodynamics Properties

Figure 4 and Table 1 show the variation of the Gibbs free energy (ΔG), Enthalpy (ΔH), Entropy (ΔS) and Heat capacity (CV) with a number of oxygen atoms at room temperature 298 K. Figure 5 and Table 2 shows the thermodynamics properties at different temperature from (298-398) K for Coronene $C_{24}$ and reduced coronene oxide $C_{24}O$-$C_{24}O_5$. It has been found that when the number of oxygen atoms increases, the system size increases and interaction between the atoms causes Gibbs free energy and enthalpy to decrease (negative sign), while with the increased temperature that ΔG decreased according to the Eq. (2), which indicate an exergonic reaction. Both the heat capacity and entropy increase with the number of oxygen atoms and temperature; this results in greater disorder within the system and a higher material temperature, as shown in the following Eqs. (2) and (3) [52,53]:

$$\Delta G=\Delta H-\Delta ST \quad (2)$$

where, ΔH is change in the enthalpy and ΔS is change in the entropy.

$$C=Q/m\Delta T \quad (3)$$

where C is heat capacity (J/(kg·K), Q is the amount of heat (in joules), m is the mass of the sample, and ΔT is the change between starting and end temperatures.

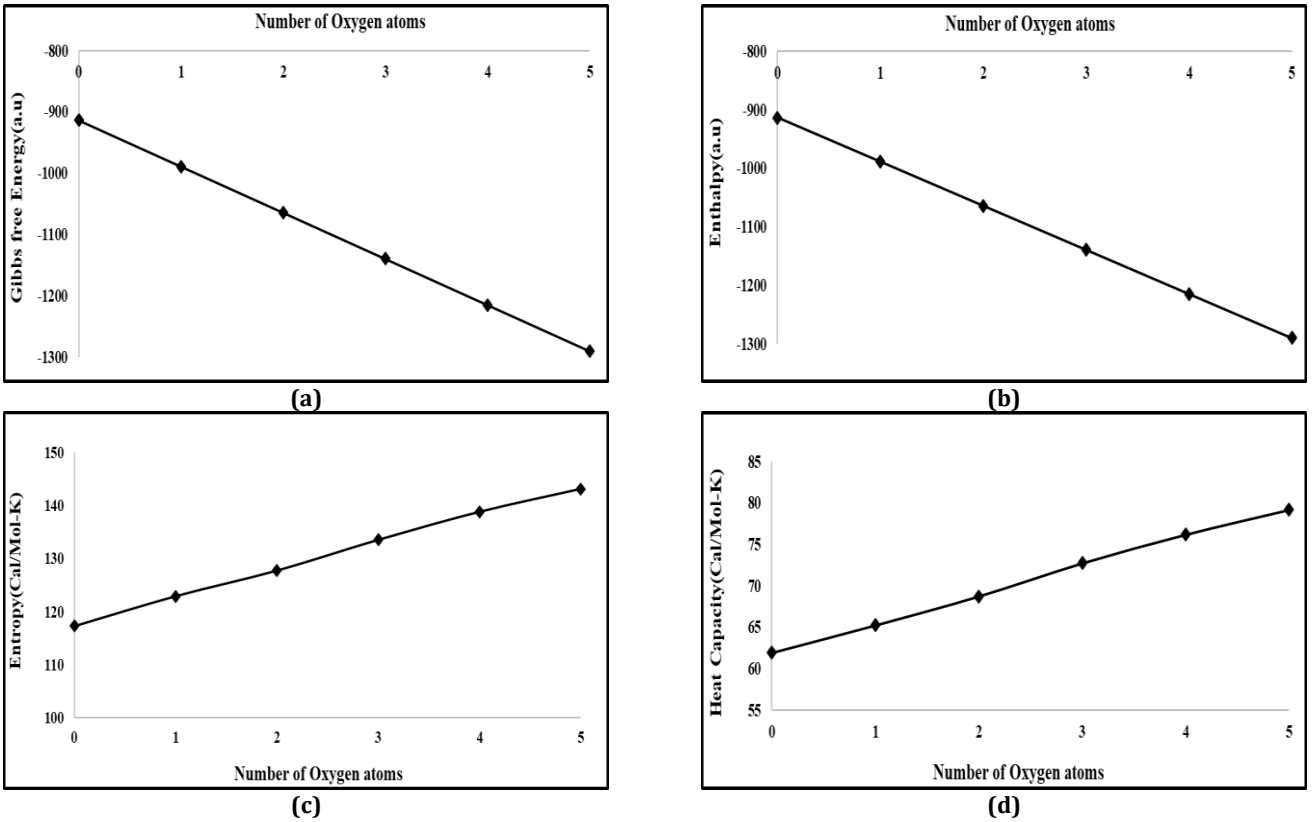


**Figure 4**. The thermodynamics properties of reduced Coronene oxide ($C_{24}O$-$C_{24}O_5$) compare with Coronene $C_{24}$ for (a) Gibbs free energy, (b) Enthalpy, (c) Entropy and (d) Heat capacity of a number of oxygen atoms

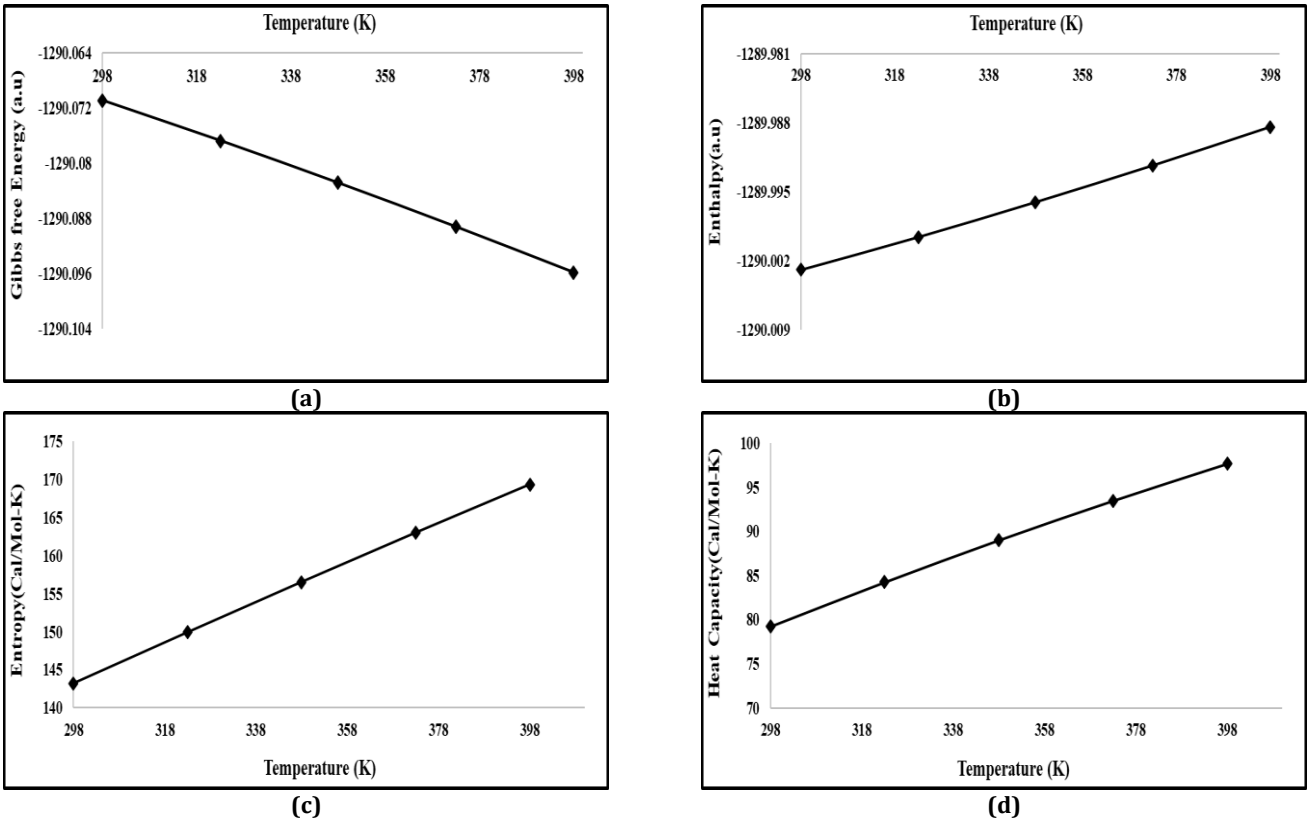


**Figure 5**. The thermodynamics properties of reduced Coronene oxide ($C_{24}O_5$) for (a) Gibbs free energy, (b) enthalpy, (c) entropy and (d) heat capacity at different temperatures

**Table 1.** The thermodynamics properties of $C_{24}$ and $C_{24}O$-$C_{24}O_5$

| Thermodynamics properties | $C_{24}$ | $C_{24}O$ | $C_{24}O_2$ | $C_{24}O_3$ | $C_{24}O_4$ | $C_{24}O_5$ |
|---|---|---|---|---|---|---|
| **ΔG (a.u)** | -913.97 | -989.20 | -1064.41 | -1139.62 | -1214.85 | -1290.07 |
| **ΔH (a.u)** | -913.92 | -989.14 | -1064.35 | -1139.55 | -1214.79 | -1290 |
| **ΔS (Cal/Mol-K)** | 117.25 | 122.91 | 127.76 | 133.57 | 138.86 | 143.20 |
| **CV (Cal/Mol-K)** | 61.92 | 65.25 | 68.74 | 72.74 | 76.20 | 79.19 |

**Table 2.** The thermodynamics properties of $C_{24}O_5$ at different temperatures from (298 - 398) K

| Thermodynamics properties | 298 K | 323 K | 348 K | 373 K | 398 K |
|---|---|---|---|---|---|
| **ΔG (a.u)** | -1290.070 | -1290.076 | -1290.082 | -1290.089 | -1290.095 |
| **ΔH (a.u)** | -1290.002 | -1289.999 | -1289.996 | -1289.992 | -1289.988 |
| **ΔS (Cal/Mol-K)** | 143.20 | 149.90 | 156.50 | 162.97 | 169.30 |
| **CV (Cal/Mol-K)** | 79.19 | 84.22 | 88.98 | 93.46 | 97.65 |

### 3.3. Spectroscopic Properties

Figure 6 and Table 3 illustrate how the intensity of the IR absorption spectra of reduced coronene oxide ($C_{24}O_5$) increases with temperature between (298 and 398) K because of an increase in the number of excited atoms according to Maxwell Boltzmann distribution, comparison with the experimental value of Longitudinal optical (LO) mode of frequency 1582 $cm^{-1}$ for graphene oxide [54].

## 4. CONCLUSIONS

Density functional theory with Hybrid functional B3LYP and 6-311G** basis sets were used to study the Coronene molecule with a variation of the number of oxygen atoms and the temperature. The obtained results can be summarized as follows.

1. The energy gap of the Coronene molecule was high because of the quantum confinement effect and Coulomb interaction.
2. It was found that the energy gap decreased with the substituting of oxygen atoms instead of hydrogen of Coronene molecule due to broken symmetry and adding level inside of the energy gap.
3. The Gibbs free energy decreased (in the negative sign) with an increase of oxygen atoms and variation of the temperature which means exergonic reaction with more stable as the definition of Gibbs free energy requires.
4. The intensity of the IR absorption spectrum of $C_{24}O_5$ was increased with increased temperature due to an increase in the number of excited atoms according to Maxwell Boltzmann distribution.

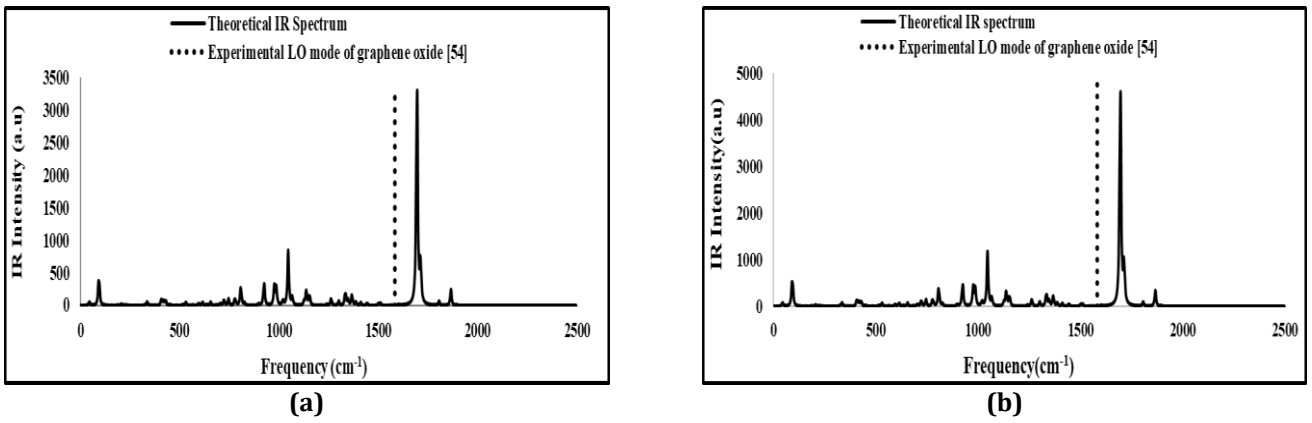


**Figure 6**. IR spectra for reduced Coronene oxide $C_{24}O_5$ as a function of frequency for (a) at 298 K and (b) at 398 k

**Table 3.** The IR intensity and frequency values of $C_{24}O_5$ at different temperatures (298 and 398) K

| Temperature (k) | IR Intensity (a.u) | Theoretical Frequency ($cm^{-1}$) | Experimental Frequency ($cm^{-1}$) [54] |
|---|---|---|---|
| **298** | 3264.46 | 1695 | 1582 |
| **398** | 4549.22 | 1695 | 1582 |

## REFERENCES

[1] E. Jennings, W. Montgomery, and P. Lerch, "Stability of Coronene at High Temperature and Pressure," *The Journal of Physical Chemistry B*, vol. 114, no. 48, pp. 15753–15758, 2010.

[2] J. C. Fetzer, *Large (C> = 24) Polycyclic Aromatic Hydrocarbons: Chemistry and Analysis*. John Wiley & Sons, 2000.

[3] F. R. Nikmaram, K. Kalateh, and P. Kanganizadeh, "The Effect of Si Substitution on Distribution of H2 on Coronene," *International Journal of New Chemistry*, vol. 1, no. 4, pp. 160–165, 2014.

[4] V. S. Zubkov, "Tendencies in the distribution and hypotheses of the genesis of condensed naphthides in magmatic rocks from various geodynamic environments," *Geochemistry International*, vol. 47, no. 8, pp. 741–757, 2009.

[5] L. J. Allamandola, S. A. Sandford, and B. Wopenka, "Interstellar Polycyclic Aromatic Hydrocarbons and Carbon in Interplanetary Dust Particles and Meteorites," *Science*, vol. 237, no. 4810, pp. 56–59, 1987.

[6] B. J. Frogley and L. J. Wright, "A Metallaanthracene and Derived Metallaanthraquinone," *Angewandte Chemie International Edition*, vol. 56, no. 1, pp. 143–147, 2017.

[7] M. Gingras, A. Pinchart, C. Dallaire, T. Mallah, and E. Levillain, "Star-Shaped Nanomolecules Based on p -Phenylene Sulfide Asterisks with a Persulfurated Coronene Core," *Chemistry – A European Journal*, vol. 10, no. 12, pp. 2895–2904, 2004.

[8] J. Cai, J. Tian, H. Gu, and Z. Guo, "Amino Carbon Nanotube Modified Reduced Graphene Oxide Aerogel for Oil/Water Separation," *ES Materials & Manufacturing*, vol. 6, pp. 68–74, 2019.

[9] H. Deng *et al.*, "Exploring the enhanced catalytic performance on nitro dyes via a novel template of flake-network Ni-Ti LDH/GO in-situ deposited with Ag3PO4 NPs," *Applied Surface Science*, vol. 543, p. 148821, 2021.

[10] A. M. Pinto, I. C. Gonçalves, and F. D. Magalhães, "Graphene-based materials biocompatibility: A review," *Colloids and Surfaces B: Biointerfaces*, vol. 111, pp. 188–202, 2013.

[11] Z. Li *et al.*, "Towards graphyne molecular electronics," *Nature Communications*, vol. 6, no. 1, p. 6321, 2015.

[12] X. Zhang *et al.*, "Synthesis, Self-Assembly, and Charge Transporting Property of Contorted Tetrabenzocoronenes," *The Journal of Organic Chemistry*, vol. 75, no. 23, pp. 8069–8077, 2010.

[13] S. Prodhan, S. Mazumdar, and S. Ramasesha, "Correlated Electronic Properties of a Graphene Nanoflake: Coronene," *Molecules*, vol. 24, no. 4, p. 730, 2019.

[14] M. F. Budyka, "Semiempirical study on the absorption spectra of the coronene-like molecular models of graphene quantum dots," *Spectrochimica Acta Part A: Molecular and Biomolecular Spectroscopy*, vol. 207, pp. 1–5, 2019.

[15] B. Saha and P. K. Bhattacharyya, "Density Functional Study on the Adsorption of 5-Membered N-Heterocycles on B/N/BN-Doped Graphene: Coronene as a Model System," *ACS Omega*, vol. 3, no. 12, pp. 16753–16768, 2018.

[16] S. Drewniak, Ł. Drewniak, and T. Pustelny, "Mechanisms of NO2 Detection in Hybrid Structures Containing Reduced Graphene Oxide: A Review," *Sensors*, vol. 22, no. 14, p. 5316, 2022.

[17] D.-T. Phan and G.-S. Chung, "P–n junction characteristics of graphene oxide and reduced graphene oxide on n-type Si(111)," *Journal of Physics and Chemistry of Solids*, vol. 74, no. 11, pp. 1509–1514, 2013.

[18] S. Alibert-Fouet, I. Seguy, J. Bobo, P. Destruel, and H. Bock, "Liquid-Crystalline and Electron-Deficient Coronene Oligocarboxylic Esters and Imides By Twofold Benzogenic Diels–Alder Reactions on

Perylenes," *Chemistry – A European Journal*, vol. 13, no. 6, pp. 1746–1753, 2007.

[19] E. H. Fort, P. M. Donovan, and L. T. Scott, "Diels–Alder Reactivity of Polycyclic Aromatic Hydrocarbon Bay Regions: Implications for Metal-Free Growth of Single-Chirality Carbon Nanotubes," *Journal of the American Chemical Society*, vol. 131, no. 44, pp. 16006–16007, 2009.

[20] K. V. Rao and S. J. George, "Synthesis and Controllable Self-Assembly of a Novel Coronene Bisimide Amphiphile," *Organic Letters*, vol. 12, no. 11, pp. 2656–2659, 2010.

[21] S. M. Omran, E. T. Abdullah, and O. A. Al-Zuhairi, "Polyvinylpyrrolidone/Multi-walled Carbon Nanotubes/Graphene Nanocomposite as Gas Sensor," *Iraqi Journal of Science*, vol. 63, no. 9, pp. 3719–3726, 2022.

[22] A. H. Mohammed, A. N. Naje, and R. k. Ibrahim, "Photoconductive Detector Based on Graphene Doping with Silver Nanoparticles," *Iraqi Journal of Science*, vol. 63, no. 12, pp. 5218–5231, 2022.

[23] A. A. Menazea *et al.*, "Chitosan/graphene oxide composite as an effective removal of Ni, Cu, As, Cd and Pb from wastewater," *Computational and Theoretical Chemistry*, vol. 1189, p. 112980, 2020.

[24] A. R. Marlinda, N. Yusoff, S. Sagadevan, and M. R. Johan, "Recent developments in reduced graphene oxide nanocomposites for photoelectrochemical water-splitting applications," *International Journal of Hydrogen Energy*, vol. 45, no. 21, pp. 11976–11994, 2020.

[25] A. K. Geim, "Graphene: Status and Prospects," *Science*, vol. 324, no. 5934, pp. 1530–1534, 2009.

[26] P. Avouris, "Graphene: Electronic and Photonic Properties and Devices," *Nano Letters*, vol. 10, no. 11, pp. 4285–4294, 2010.

[27] F. Schwierz, "Graphene transistors," *Nature Nanotechnology*, vol. 5, no. 7, pp. 487–496, 2010.

[28] L. M. Viculis, J. J. Mack, and R. B. Kaner, "A Chemical Route to Carbon Nanoscrolls," *Science*, vol. 299, no. 5611, pp. 1361–1361, 2003.

[29] C. Berger *et al.*, "Ultrathin Epitaxial Graphite: 2D Electron Gas Properties and a Route toward Graphene-based Nanoelectronics," *The Journal of Physical Chemistry B*, vol. 108, no. 52, pp. 19912–19916, 2004.

[30] T. A. Land, T. Michely, R. J. Behm, J. C. Hemminger, and G. Comsa, "STM investigation of single layer graphite structures produced on Pt(111) by hydrocarbon decomposition," *Surface Science*, vol. 264, no. 3, pp. 261–270, 1992.

[31] J. P. Almeida de Mendonça *et al.*, "Structural and vibrational study of graphene oxide via coronene based models: theoretical and experimental results," *Materials Research Express*, vol. 3, no. 5, p. 055020, 2016.

[32] M. L. Jabbar, "Some electronical properties for Coronene-Y interactions by using density functional theory (DFT)," *Journal of Basrah Researches (Sciences)*, vol. 44, no. 1A, pp. 11–19, 2018.

[33] H. Asadi, K. Zhour, and A. Zavartorbati, "DFT study of Benzene, Coronene and Circumcoronene as zigzag graphene quantum dots," *Journal of Interface, Thin Film and Low Dimension Systems*, vol. 3, no. 1, pp. 203–210, 2019.

[34] S. K. Abdulradha, M. T. Hussein, and M. A. Abdulsattar, "Study of the Interaction Between Reduced Graphene Oxide and NO 2 Gas Molecules via Density Functional Theory (DFT)," *International Journal of Nanoscience*, vol. 21, no. 02, p. 2250009, 2022.

[35] M. A. Hadi and M. T. Hussein, "Study the Effect of Oxygen on Coronene Electronic and Spectroscopic Properties via the Density Functional Theory (DFT)," *Iraqi Journal of Science*, vol. 64, no. 1, pp. 157–165, 2023.

[36] P. J. Stephens, F. J. Devlin, C. F. Chabalowski, and M. J. Frisch, "Ab Initio Calculation of Vibrational Absorption and Circular Dichroism Spectra Using Density Functional Force Fields," *The Journal of Physical Chemistry*, vol. 98, no. 45, pp. 11623–11627, 1994.

[37] K. Kim and K. D. Jordan, "Comparison of Density Functional and MP2 Calculations on the Water Monomer and Dimer," *The Journal of Physical Chemistry*, vol. 98, no. 40, pp. 10089–10094, 1994.

[38] M. T. Hussein, T. Kasim, and M. A. Abdulsattar, "First principle study of electronic nanoscale structure of In x Ga1−x P with variable size, shape and alloying percentage," *Indian Journal of Physics*, vol. 87, no. 11, pp. 1079–1085, 2013.

[39] S. K. Abdulradha, M. T. Hussein, and M. A. Abdulsattar, "Study the Electronic and Spectroscopic Characteristics of p-n Heterojunction Hybrid (Sn10O16/C24O6) via Density Functional Theory (DFT)," *Iraqi Journal of Physics*, vol. 21, no. 3, pp. 24–32, 2023.

[40] M. T. Hussein, "First principles calculations of Al AsxP1-x ternary nanocrystal alloying composition," *Iraqi Journal of Physics*, vol. 15, no. 33, pp. 54–62, 2019.

[41] S. K. Abdulridha, M. A. Abdulsattar, and M. T. Hussein, "Sensitivity of SnO2 nanoparticles/reduced graphene oxide hybrid to NO2 gas: a DFT study," *Structural Chemistry*, vol. 33, no. 6, pp. 2033–2041, 2022.

[42] Q. X. Zhou, Z. B. Fu, C. Y. Wang, X. Yang, L. Yuan, and Y. J. Tang, "Electronic and Magnetic Properties of Rare-Earth Atoms Absorbed on Graphene Sheet: A Theoretical Study," *Key Engineering Materials*, vol. 645–646, pp. 40–44, 2015.

[43] M. A. Abdulsattar, H. H. Abed, R. H. Jabbar, and N. M. Almaroof, "Effect of formaldehyde properties on SnO2 clusters gas sensitivity: A DFT study," *Journal of Molecular Graphics and Modelling*, vol. 102, p. 107791, 2021.

[44] N. Sieffert and G. Wipff, "Uranyl extraction by N,N-dialkylamide ligands studied using static and dynamic DFT simulations," *Dalton Transactions*, vol. 44, no. 6, pp. 2623–2638, 2015.

[45] M. T. Hussein, T. A. Fayad, and M. A. Abdulsattar, "Concentration effects on electronic and spectroscopic properties of ZnCdS wurtzoids: A density functional theory study," *Chalcogenide Letters*, vol. 16, no. 11, pp. 557–563, 2019.

[46] M. T. Hussein and H. A. Thjeel, "Vibration Properties of ZnS nanostructure Wurtzoids: ADFT Study," in *Journal of Physics: Conference Series*, 2019, p. 012015.

[47] A. H. Taha, "Electronic Structure Simulation of Aluminum Antimony Nanocrystal Using Ab-initio Density Functional Theorycoupled with Large Unit Cell Method," *American Journal of Condensed Matter Physics*, vol. 4, no. 4, pp. 63–70, 2014.

[48] H. Tian *et al.*, "Wafer-Scale Integration of Graphene-based Electronic, Optoelectronic and Electroacoustic Devices," *Scientific Reports*, vol. 4, no. 1, p. 3598, 2014.

[49] E. C. Mattson *et al.*, "Vibrational Excitations and Low-Energy Electronic Structure of Epoxide-Decorated Graphene," *The Journal of Physical Chemistry Letters*, vol. 5, no. 1, pp. 212–219, 2014.

[50] H. Liang, "Mid-infrared response of reduced graphene oxide and its high-temperature coefficient of resistance," *AIP Advances*, vol. 4, no. 10, p. 107131, 2014.

[51] L. Yang, C.-H. Park, Y.-W. Son, M. L. Cohen, and S. G. Louie, "Quasiparticle Energies and Band Gaps in Graphene Nanoribbons," *Physical Review Letters*, vol. 99, no. 18, p. 186801, 2007.

[52] C.-S. Jia *et al.*, "Prediction of entropy and Gibbs free energy for nitrogen," *Chemical Engineering Science*, vol. 202, pp. 70–74, 2019.

[53] M. Popovic, G. B. G. Stenning, A. Göttlein, and M. Minceva, "Elemental composition, heat capacity from 2 to 300 K and derived thermodynamic functions of 5 microorganism species," *Journal of Biotechnology*, vol. 331, pp. 99–107, 2021.

[54] Y. Shen *et al.*, "Evolution of the band-gap and optical properties of graphene oxide with controllable reduction level," *Carbon*, vol. 62, pp. 157–164, 2013.